# 710 kW stable average-power in a 45,000 finesse two-mirror optical cavity

XIN-YI LU[1,2], RONIC CHICHE[1], KEVIN DUPRAZ[1], AURÉLIEN MARTENS[1,*], DANIELE NUTARELLI[1], VIKTOR SOSKOV[1], FABIAN ZOMER[1], XING LIU[2], LI-XIN YAN[2], WEN-HUI HUANG[2], CHUAN-XIANG TANG[2], CHRISTOPHE MICHEL[3], LAURENT PINARD[3], AND JÉRÔME LHERMITE[4]

[1] *Université Paris-Saclay, CNRS/IN2P3, IJCLab, 91405 Orsay, France.*
[2] *Department of Engineering Physics, Tsinghua University, Beijing 100084, China.*
[3] *Laboratoire des Matériaux Avancés - IP2I, CNRS, Université de Lyon, Université Claude Bernard Lyon 1, F-69622 Villeurbanne, France.*
[4] *Université de Bordeaux - CNRS-CEA, Centre Lasers Intenses et Applications (CELIA), 351 cours de la Libération F-33405 Talence, France.*
[*] *aurelien.martens@ijclab.in2p3.fr*

*Compiled November 4, 2024*

**Very-high average optical enhancement cavities are being used both in fundamental and applied research. The most demanding applications require stable megawatt level average power of infrared picosecond pulses with repetition rates of several tens of MHz. Towards reaching this goal, we report on the achievement of 710 kW of stable average power in a two-mirror hemispherical optical enhancement cavity. This result further improves on the state of the art. We observed the influence of thermal lensing induced by residual absorption in the coating. This is observed for the first time in this context, though the effect was well predicted in literature. Experimental observations are matched with a simple model of thermal effects in the mirror's coatings. These results set a further stage to design an optimized optical system for several applications where very high average-power enhancement cavities are expected to be operated.**

http://dx.doi.org/10.1364/ao.XX.XXXXXX

Very high average-power optical enhancement cavities (OEC) are being used for instance in high-harmonic generation [1], gravitational waves observatories [2], compact radiation sources [3–5] and for interaction with ion beams [6]. Improving on the present state of the art would allow further applications as photo-neutralization of deuterium for fusion energy experiments [7] and steady-state micro-bunching which is foreseen for the production of high-peak and high-average power of EUV radiation [8].

Up to 670 kW average power in a four-mirror bow-tie OEC was obtained ten years ago with 10 picosecond pulses at a 250 MHz repetition rate with a sapphire input mirror of the cavity [9]. Since this work was tailored to high-harmonic generation, the investigators reduced pulse duration down to 250 fs and obtained 400 kW with a fused silica input coupler. In this work a high-average power laser amplifier delivering up to 420 W was used and the OEC had an effective enhancement factor of 2000 decreasing to 1200 at high input average power. These experiments exhibited large OEC mode deformation related to the residual coating absorption that induces thermal deformation of the mirror surfaces and in turn a modification of the OEC topology. Design constraints for future implementation of OEC were drawn [10]. Indeed, operating the OEC closer to the instability region induces larger mode deformation per unit of average power stored in the cavity [9, 11].

Mirror deformation of OEC further induces instabilities related to the degeneracy of high-order modes with the fundamental one [12]. It induces variation of the stored power but also loss of the feedback in between the laser and the OEC. This effect was mitigated in the context of the development of OEC for compact light sources by inserting a pair of high order mode dampers in the OEC [13]. It allowed to reach stable 200 kW in a four-mirror bow-tie cavity. Recent improvements in the mirror coating, and availability of laser oscillator with unprecedented phase stability allowed us to demonstrate stable 500 kW operation in a 35,000 finesse cavity with effective enhancement factor of 8,000 [11]. It must be emphasized that in this work, a very high-average power of infrared light was stacked with input power reduced by a factor six compared to the work shown in Ref. [9], thus allowing an interesting cost and footprint reduction for operation in accelerator environment. Maximum available amplifier power and performance hindered further improvements. This limitation is partly overcome here by increasing further the enhancement factor of the OEC.

These developments were made with 4-mirror bow-tie OECs particularly well suited for compact light sources [14]. Indeed, the ability to adjust independently the laser focus at the interaction point with a focused electron beam is critical to optimize the interaction rate and the OEC length to match the electron beam revolution frequency [15]. However, interaction with a nearly collimated electron beam, as considered for the SSMB project [8], or with a hadronic beam in the Gamma Factory Proof of principle [6] allow considering two-mirror OEC either in a hemispherical or confocal geometry. With a given mirror coating performance it would induce an increase in the finesse and the enhancement factor of the OEC but mode degeneracy would still appear. In this letter, we aim at investigating the performance of a hemispherical OEC in the preparation of these projects and, as a by product, to further improve on high-average power performance of OECs. In particular one of the goal is to look for further possible scaling limitations that could be induced by significantly increased intensity on mirrors.

To that purpose, we implement a very similar setup as that described in Ref. [11], shown in Fig. 1, except that, due to space limitation in the vacuum chamber used for these experimental developments, the cavity free-spectral range and laser seeder repetition rate are 216.66 MHz. The pulse duration is about 160 ps and laser wavelength centred at 1030 nm [11]. A two-lens telescope in implemented, with focal lengths and distances adjusted throughout the experiment to improve performance at higher power. Since injection is nominally made with normal incidence, a polarizing beam splitter and quarter-wave plate are used to direct the OEC reflection field to a photodiode for the Pound-Drever-Hall locking technique [16]. Mirrors from the same batches as those used in Ref. [11] are implemented in the OEC. The input Suprasil 3001 mirror $M_1$ is planar with a transmission of $113 \pm 1$ ppm, where ppm denotes a part per million. The output coupler $M_2$ is made of Corning ULE with a radius of curvature of 2.241 m and exhibit a measured transmission of $1.75 \pm 0.01$ ppm. The distance in between the mirrors is of approximately 0.69 m and adjusted with motorized stage to the repetition rate of the seed laser. The employed geometry induces a small beam radius at $e^{-2}$ of intensity on the mirrors of 0.58 (0.70) mm on $M_1$ ($M_2$). This beam size is about a factor two smaller than that needed for the Gamma Factory Proof of Principle experiment [6]. It however allows increasing by a factor at least nine compared to past studies [11] the laser intensity on the mirror coatings and the sensitivity to thermal effects which scale as the square of the beam radius. This is an important feature of this setup to probe, with reduced average power, effects that will appear at higher average power with larger beam size in future experiments. In this experiment one also investigates for the first time the operation of 2-mirror cavity at very high average power.

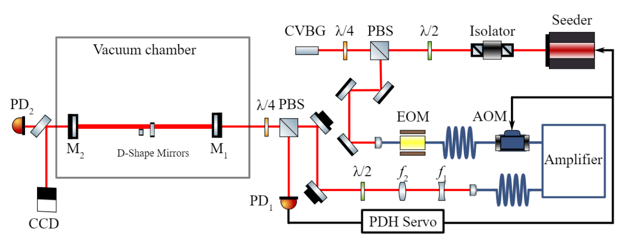


**Fig. 1.** Schematic of the experimental setup used for the experiments described in this Letter. EOM stands for electro-optic modulator; AOM stands for acousto-optic modulator; PBS for polarizing beam splitter; CVBG for chirped volume Bragg grating; PDH for Pound–Drever–Hall; PD for photodiode; CCD is a beam profiler.

The finesse is measured to be of $45,000 \pm 2,000$ [11, 17]. To the best of our knowledge, this is the highest finesse implemented in the context of high average power OECs. Given the measured mirrors' transmissions, it provides an estimate for additional losses to be of $25 \pm 4$ ppm due to scattering since coating absorption is below 0.6 ppm. The corresponding linewidth of the OEC is of 4.8 kHz. The telescope is first optimized to best match the cold (low power) OEC mode. With 10.4 W of input power, 191 kW can be stacked in the OEC, exhibiting an 18,400 effective enhancement factor that is the product of the ideal OEC enhancement factor and coupling $C$ that accounts for residual misalignments, mode mismatching and phase noise. The average power and the beam profile 0.67 m are measured downstream $M_2$ during experiments. Increasing the amplifier average power allowed to reach up to 500 kW of average power in the cavity with a saturation at this level for about 30 W input power, see the red squares labelled first run on the Fig. 2. The measurement of the beam size in transmission of $M_2$ is given in Fig. 3. It clearly shows a large beam size reduction as a function of the stored average power. This result may be found surprising at first glance, since the change of the radii of curvature of the OEC mirrors due to thermal loading [18, 19] would rather induce a slight increase in the size of the measured beam spot, see the full black line in Fig. 3. The paraxial approximation and ABCD matrix formalism [20, 21] was employed in the calculations. It affects the operation of OECs close to instability region with large beam size on mirrors [9, 11], but does not intervene in the OEC far from instability reported in this Letter.

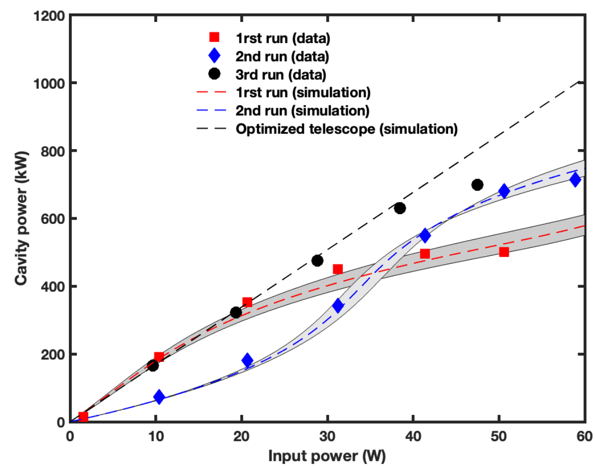


**Fig. 2.** The average power stacked in the OEC as a function of the input average power.

The explanation for the measured beam size actually lies in the occurrence of thermal lensing in the substrate of $M_2$. Thermal lensing is a well known effect in high average power, see for instance Ref. [22] for a review. In OECs there is however restricted literature. It is mostly related to work made in the context of gravitational wave detectors [23] where countermeasures were considered [24–26]. Thermal lensing induced by unit length absorption of laser intensity in materials is extensively studied in these works. In the work presented here, thermal lensing is induced by the heat gradient in the substrate generated by the small residual absorption $a < 0.6ppm$ of mirror coatings [27] under a high-average optical power $P_c$. It is mentioned in literature [18, 19], but was never observed experimentally yet to the best of our knowledge. Under paraxial approximation, the effect can be modelled by a $P_c$ dependant focal length $f_i$, for mirror $M_i$, that reads $f_i^{-1} = \beta_i a_i P_c / (\pi \kappa_i w_i^2)$ where $a_i$ the absorption coefficient of the coating of the $i$-th mirror. The thermal conductivities are taken to be $\kappa_1 = 1.38 W.m^{-1}.K^{-1}$ and $\kappa_2 = 1.31 W.m^{-1}.K^{-1}$. The thermo-optic coefficient of the bulk is taken to be $\beta_1 = 8.1 \cdot 10^{-6}\mathrm{K}^{-1}$ and $\beta_2 = 10.7 \cdot 10^{-6}\mathrm{K}^{-1}$for

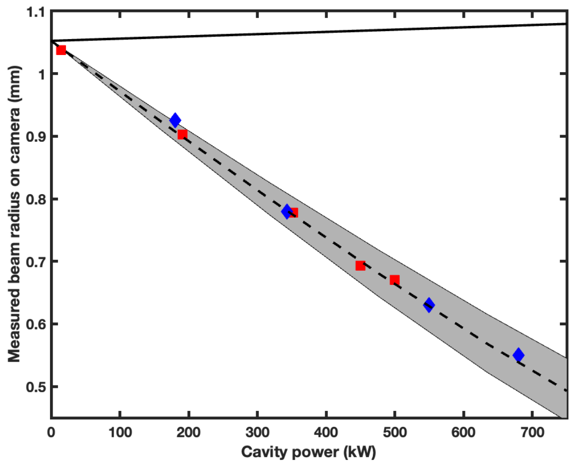


**Fig. 3.** The beam radius (at $1/e^2$ of intensity profile), measured on a camera 67 cm downstream the output mirror, as a function of the average power in the OEC. Points in red and blue show measurements made during the first and second run showing excellent consistency. The black solid line is the expected beam radius on the camera only accounting for the change of ROC of the mirrors due to thermal loading of the OEC. The dashed line further accounts for thermal lensing in the bulk of $M_2$ assuming a coating absorption of 0.36 ppm, as explained in the text. The grey band represents a variation of the coating absorption by about 10%.

Suprasil and ULE, respectively [18]. We checked that it corresponds to approximate the optical path distortion inside the heated substrate of Hello-Vinet model [19] by a parabola. This approximation is found good over the beam radius and sufficient to model the observed data. The beam size computed accounting for the $P_c$-dependent thermal lensing is shown in Fig. 3 in dashed line for $a = 0.36$ ppm. This initially poorly known value has been adjusted to provide a result consistent with measured data. Unfortunately the assumed value for the thermo-optic coefficient of ULE is subject to caution since it is related to $TiO_2$ concentration that varies sufficiently to induces variation of this coefficient by several percents [28]. It justifies some 10% uncertainty on the estimation of $\beta_2$, inducing in turn a similar uncertainty on the coating absorption $a$. A grey band corresponding to the variation of $a$ in the range $a = 0.33 - 0.39$ ppm is draw. It must be noted that this value of absorption is consistent with the independently measured value of transmission and an approximate model for these quantities [27, 29, 30]. It provides an interesting self-consistent picture. The observed beam shape is shown on Fig. 4 for a power in the cavity of approximately 650 kW. It must be noted that the beam has a clean Gaussian shape. No sign of residual higher order mode is observed. Indeed, intracavity high-order mode dampers in the form of D-shape mirrors have been implemented and tuned to minimize the influence of mode degeneracies [11, 13].

Thermal lensing also affects the coupling of the laser beam to the OEC. A simulation, under paraxial approximation, of the optimum waist position (relative to the position of $M_1$) and size is shown in Fig. 5. Contours representing the allowed region in this plane to preserve 90% of coupling coefficient related to transverse mode-matching are shown. Their areas strongly reduce with increasing power, implying a more difficult telescope

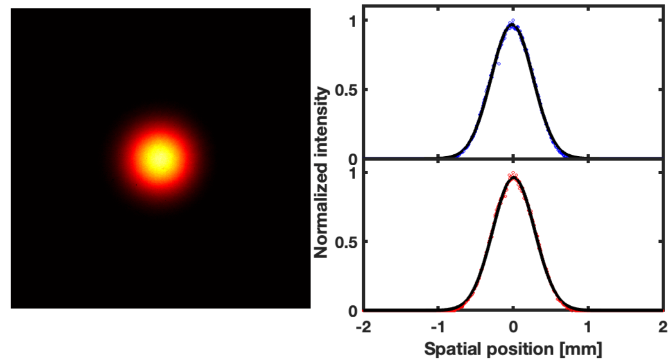


**Fig. 4.** (Left) Beam profile as measured on the camera at 650 kW. (Right) corresponding projections in the horizontal (up) and vertical (down) axes are given with coloured dots. The black line is a Gaussian fit of these data. The beam remain circular with no obvious presence of high order mode degeneracy.

tuning. This has been well observed in the experiments and validated with simulations of the employed two-lens telescope. This first run exhibited a clear saturation of the power inside the optical cavity at about 500 kW, see Fig. 2, which can be qualitatively explained by the strong mismatch of the telescope to the power loaded cavity.Indeed, the region in waist size and position to get good mode-matching to the OEC at 500 kW is nearly disconnected to that at 100 kW, see Fig. 5.

The telescope design has been adapted by means of simulations, accounting for the observed thermal lensing effect, with the goal to reach 700 kW. The measured data is shown in blue diamonds in Figs. 2-3. Up to 710 kW of average power is obtained, with stable operation for fifteen minutes. The cavity was stably operated as in a previous study [11]. Below 35 W of input power, the cavity mode matching is worse than for the first run. The OEC average power however improves on the first run above 40W of input power, exhibiting a relatively well adapted telescope. This behaviour can be well explained by simulations assuming that $C = 0.63$ and that absorption in the input mirror is of 0.56 ppm. The light grey band corresponds to curves obtained at 0.52 and 0.60 ppm $M_1$ absorption, respectively. Changing the assumption on the value of $C$ or slightly changing lenses positions in the simulation by a few millimetres does not affect significantly this result. Assuming 0.56 ppm absorption for $M_1$ and looking for the best parameters for ideal coupling coefficient $C$ and first run telescope parameters varied within few millimetres around the expected nominal position, provides the red dashed line. For the obtained value of $C$, the grey band represents a variation of the relative position of the two lenses of the telescope by $\pm 3$ mm. The result suggests some excess absorption in $M_1$ compared to $M_2$, which is from a different coating batch with $113 \pm 1$ ppm transmission. Finally, we decided to empirically tune the telescope while raising the cavity power. This result is shown with black dots in Fig. 2. We obtained a significant improvement in the behaviour of the intra-cavity power as function of the input power, close to a linear curve shown in dashed. The effective enhancement factor is of 16,400 up to a 38.5 W input power. This reduced enhancement factor compared to the first run may be explained by a telescope a bit worse optimized at the start. A decrease of 10% of the effective enhancement is observed at 47.5 W. At such high average power of 700 kW the telescope could not be improved

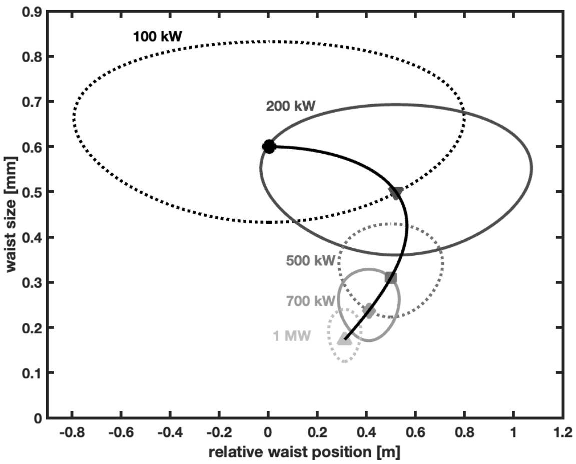


**Fig. 5.** Simulation of the optimum waist size versus optimum waist position of the input laser beam relative to the input mirror, accounting for thermal lensing in $M_1$ (solid black line and dots). Encircled regions corresponding to coupling coefficient related to transverse mode-matching in excess of 90% for 100 kW, 200 kW, 500 kW and 1 MW in this plane, with their optimum shown with a marker. The $M_1$ mirror absorption is assumed to be of $a_1 = 0.56$ ppm.

with success. Explanation lies in a very restricted region of parameter space allowed for the implemented telescope to reach a good enough matching of the input beam to the OEC mode, as shown in Fig. 5. A more detailed study is deserved, with systematic measurements and more telescope configurations to allow a more accurate estimation of the absorption coefficient. This is kept for a further study, out of the scope of this Letter. The overall good consistency of the measurements is however striking.

Demonstration of stable 710kW of average power of infrared light in a 2-mirror 45,000 finesse optical enhancement cavity is made. This is the highest average power laser system demonstrated so far. Effective enhancement up to 18,400 was obtained, which is the largest demonstrated to date in high average power regime. As a by product, we could obtain about 200 kW of average power with about 11 W input laser power, which is of particular interest for the Gamma Factory proof of principle experiment [6]. It allows a drastic reduction of the scale of the laser amplifier for Compton scattering based radiation sources or for other accelerator based applications, that would induce a significant cost reduction in such systems. For the first time in this context, an OEC is operated in a regime where spot sizes on mirror are small and non-linearities mainly due to thermal lensing. The observed behaviour is reasonably well reproduced by simulations and provides some interesting sensitivity to the actual absorption level in the mirror coatings well below one part per million. Further detailed, more systematic, studies are in order to provide accurate estimates, that are left outside the scope of this paper. This result sets a new stage towards average power in excess of 1 MW, which will open new accelerator based applications for these devices.

**Funding.** The present work is partially financed by the French National Research Agency (ANR) under the Equipex program ANR-10-EQPX-0051. The authors also acknowledge the funding of CERN Physics Beyond Collider initiative. X.-Y. Lu stays at IJCLab was funded by National Key Research and Development Program of China (Grant No. 2022YFA1603403).

**Acknowledgments.** The authors also acknowledge the support of the France-China Particle Physics Network which provided to the IJCLab and Tsinghua University teams a frame for fruitful exchanges over the past years.

**Disclosures.** The authors declare no conflicts of interest.

**Data Availability Statement.** Data underlying the results presented in this paper are not publicly available at this time, but may be obtained from the authors upon reasonable request.

## REFERENCES

1. I. Pupeza, S. Holzberger, T. Eidam, *et al.*, Nat. Photonics **7**, 608 (2013).
2. D. Ganapathy, W. Jia, M. Nakano *et al.*, Phys. Rev. X **13**, 041021 (2023).
3. Z. Huang and R. D. Ruth, Phys. Rev. Lett. **80**, 976 (1998).
4. B. Günther, R. Gradl, C. Jud *et al.*, J. Synchrotron Radiat. **27**, 1395 (2020).
5. M. Jacquet, P. Alexandre, M. Alkadi, *et al.*, The Eur. Phys. J. Plus **139**, 459 (2024).
6. A. Martens, K. Cassou, R. Chiche *et al.*, Phys. Rev. Accel. Beams **25**, 101601 (2022).
7. M. Tran, P. Agostinetti, G. Aiello *et al.*, Fusion Eng. Des. **180**, 113159 (2022).
8. Z. Li, X. Deng, Z. Pan *et al.*, Phys. Rev. Accel. Beams **26**, 110701 (2023).
9. H. Carstens, N. Lilienfein, S. Holzberger *et al.*, Opt. Lett. **39**, 2595 (2014).
10. H. Carstens, *Megawatt-Level Average Power Enhancement Cavities for Ultrashort Pulses* (Springer International Publishing, Cham, 2018), pp. 47–64.
11. X.-Y. Lu, R. Chiche, K. Dupraz, *et al.*, Appl. Phys. Lett. **124**, 251105 (2024). _eprint: https://pubs.aip.org/aip/apl/article-pdf/doi/10.1063/5.0213842/20005067/251105_1_5.0213842.pdf.
12. A. L. Bullington, B. T. Lantz, M. M. Fejer, and R. L. Byer, Appl. Opt. **47**, 2840 (2008).
13. L. Amoudry, H. Wang, K. Cassou *et al.*, Appl. Opt. **59**, 116 (2020).
14. F. Zomer, Y. Fedala, N. Pavloff *et al.*, Appl. Opt. **48**, 6651 (2009).
15. I. Chaikovska, K. Cassou, R. Chiche *et al.*, Sci. Reports **6**, 36569 (2016).
16. R. W. P. Drever, J. L. Hall, F. V. Kowalski *et al.*, Appl. Phys. B **31**, 97 (1983).
17. C. R. Locke, D. Stuart, E. N. Ivanov *et al.*, Opt. Express **17**, 21935 (2009).
18. W. Winkler, K. Danzmann, A. Rüdiger, and R. Schilling, Phys. Rev. A **44**, 7022 (1991).
19. Hello, Patrice and Vinet, Jean-Yves, J. Phys. France **51**, 1267 (1990).
20. H. Kogelnik and T. Li, Appl. optics **5**, 1550 (1966).
21. A. E. Siegman, *Lasers* (University science books, 1986).
22. K. Dobek, Appl. Phys. B **128**, 18 (2022).
23. K. Strain, K. Danzmann, J. Mizuno, *et al.*, Phys. Lett. A **194**, 124 (1994).
24. C. Zhao, J. Degallaix, L. Ju, *et al.*, Phys. Rev. Lett. **96**, 231101 (2006).
25. Y. Fan, C. Zhao, J. Degallaix, *et al.*, Rev. Sci. Instruments **79**, 104501 (2008). _eprint: https://pubs.aip.org/aip/rsi/article-pdf/doi/10.1063/1.2982239/14827186/104501_1_online.pdf.
26. C. Justin Kamp, H. Kawamura, R. Passaquieti, and R. DeSalvo, Nucl. Instruments Methods Phys. Res. Sect. A: Accel. Spectrometers, Detect. Assoc. Equip. **607**, 530 (2009).
27. C. Comtet, D. Forest, P. Ganau *et al.*, “Reduction of tantala mechanical losses in Ta2O5/SiO2 coatings for the next generation of VIRGO and LIGO interferometric gravitational waves detectors,” in *42th Rencontres de Moriond - Gravitational Waves and Experimental Gravity*, (La Thuile, Italy, 2007).
28. “Private communication with corning incorporated,” .
29. M. Sparks, J. Opt. Soc. Am. **67**, 1590 (1977).
30. H. E. Bennett and D. K. Burge, J. Opt. Soc. Am. **70**, 268 (1980).

## FULL REFERENCES


1. I. Pupeza, S. Holzberger, T. Eidam, *et al.*, “Compact high-repetition-rate source of coherent 100 eV radiation,” Nat. Photonics **7**, 608–612 (2013).
2. D. Ganapathy, W. Jia, M. Nakano *et al.*, “Broadband quantum enhancement of the ligo detectors with frequency-dependent squeezing,” Phys. Rev. X **13**, 041021 (2023).
3. Z. Huang and R. D. Ruth, “Laser-electron storage ring,” Phys. Rev. Lett. **80**, 976–979 (1998).
4. B. Günther, R. Gradl, C. Jud *et al.*, “The versatile X-ray beamline of the Munich Compact Light Source: design, instrumentation and applications,” J. Synchrotron Radiat. **27**, 1395–1414 (2020).
5. M. Jacquet, P. Alexandre, M. Alkadi, *et al.*, “First production of X-rays at the ThomX high-intensity Compton source,” The Eur. Phys. J. Plus **139**, 459 (2024).
6. A. Martens, K. Cassou, R. Chiche *et al.*, “Design of the optical system for the gamma factory proof of principle experiment at the cern super proton synchrotron,” Phys. Rev. Accel. Beams **25**, 101601 (2022).
7. M. Tran, P. Agostinetti, G. Aiello *et al.*, “Status and future development of heating and current drive for the eu demo,” Fusion Eng. Des. **180**, 113159 (2022).
8. Z. Li, X. Deng, Z. Pan *et al.*, “Generalized longitudinal strong focusing in a steady-state microbunching storage ring,” Phys. Rev. Accel. Beams **26**, 110701 (2023).
9. H. Carstens, N. Lilienfein, S. Holzberger *et al.*, “Megawatt-scale average-power ultrashort pulses in an enhancement cavity,” Opt. Lett. **39**, 2595–2598 (2014).
10. H. Carstens, *Megawatt-Level Average Power Enhancement Cavities for Ultrashort Pulses* (Springer International Publishing, Cham, 2018), pp. 47–64.
11. X.-Y. Lu, R. Chiche, K. Dupraz, *et al.*, “Stable 500 kW average power of infrared light in a finesse 35 000 enhancement cavity,” Appl. Phys. Lett. **124**, 251105 (2024). _eprint: https://pubs.aip.org/aip/apl/article-pdf/doi/10.1063/5.0213842/20005067/251105_1_5.0213842.pdf.
12. A. L. Bullington, B. T. Lantz, M. M. Fejer, and R. L. Byer, “Modal frequency degeneracy in thermally loaded optical resonators,” Appl. Opt. **47**, 2840–2851 (2008).
13. L. Amoudry, H. Wang, K. Cassou *et al.*, “Modal instability suppression in a high-average-power and high-finesse fabry–perot cavity,” Appl. Opt. **59**, 116–121 (2020).
14. F. Zomer, Y. Fedala, N. Pavloff *et al.*, “Polarization induced instabilities in external four-mirror fabry-perot cavities,” Appl. Opt. **48**, 6651–6661 (2009).
15. I. Chaikovska, K. Cassou, R. Chiche *et al.*, “High flux circularly polarized gamma beam factory: coupling a Fabry-Perot optical cavity with an electron storage ring,” Sci. Reports **6**, 36569 (2016).
16. R. W. P. Drever, J. L. Hall, F. V. Kowalski *et al.*, “Laser phase and frequency stabilization using an optical resonator,” Appl. Phys. B **31**, 97–105 (1983).
17. C. R. Locke, D. Stuart, E. N. Ivanov *et al.*, “A simple technique for accurate and complete characterisation of a fabry-perot cavity,” Opt. Express **17**, 21935–21943 (2009).
18. W. Winkler, K. Danzmann, A. Rüdiger, and R. Schilling, “Heating by optical absorption and the performance of interferometric gravitational-wave detectors,” Phys. Rev. A **44**, 7022–7036 (1991).
19. Hello, Patrice and Vinet, Jean-Yves, “Analytical models of thermal aberrations in massive mirrors heated by high power laser beams,” J. Phys. France **51**, 1267–1282 (1990).
20. H. Kogelnik and T. Li, “Laser beams and resonators,” Appl. optics **5**, 1550–1567 (1966).
21. A. E. Siegman, *Lasers* (University science books, 1986).
22. K. Dobek, “Thermal lensing: outside of the lasing medium,” Appl. Phys. B **128**, 18 (2022).
23. K. Strain, K. Danzmann, J. Mizuno, *et al.*, “Thermal lensing in recycling interferometric gravitational wave detectors,” Phys. Lett. A **194**, 124–132 (1994).
24. C. Zhao, J. Degallaix, L. Ju, *et al.*, “Compensation of strong thermal lensing in high-optical-power cavities,” Phys. Rev. Lett. **96**, 231101 (2006).
25. Y. Fan, C. Zhao, J. Degallaix, *et al.*, “Feedback control of thermal lensing in a high optical power cavity,” Rev. Sci. Instruments **79**, 104501 (2008). _eprint: https://pubs.aip.org/aip/rsi/article-pdf/doi/10.1063/1.2982239/14827186/104501_1_online.pdf.
26. C. Justin Kamp, H. Kawamura, R. Passaquieti, and R. DeSalvo, “Directional radiative cooling thermal compensation for gravitational wave interferometer mirrors,” Nucl. Instruments Methods Phys. Res. Sect. A: Accel. Spectrometers, Detect. Assoc. Equip. **607**, 530–537 (2009).
27. C. Comtet, D. Forest, P. Ganau *et al.*, “Reduction of tantala mechanical losses in Ta2O5/SiO2 coatings for the next generation of VIRGO and LIGO interferometric gravitational waves detectors,” in *42th Rencontres de Moriond - Gravitational Waves and Experimental Gravity,* (La Thuile, Italy, 2007).
28. “Private communication with corning incorporated,” .
29. M. Sparks, “A simple method for calculating the optical properties of multilayer-dielectric reflectors∗,” J. Opt. Soc. Am. **67**, 1590–1594 (1977).
30. H. E. Bennett and D. K. Burge, “Simple expressions for predicting the effect of volume and interface absorption and of scattering in high-reflectance or antireflectance multilayer coatings,” J. Opt. Soc. Am. **70**, 268–276 (1980).